Chapter 11

MULTISCALE SOIL EROSION SIMULATIONS FOR LAND USE MANAGEMENT

Helena Mitasova[1] and Lubos Mitas[2]
[1] *University of Illinois at Urbana-Champaign;* [2] *North Carolina State University*

1. INTRODUCTION

Increasing pressures on the land and an improved understanding of human impacts on the environment are leading to profound changes in land management, with emphasis on integration of local actions with watershed-scale approaches. This trend has a significant impact on the development of supporting *GIS* and modeling tools. Complex, distributed, physics-based models are needed to improve understanding and prediction of landscape processes at any point in space and time. At the same time, land owners and managers working in the watersheds and fields need fast and easy to use models for which the input data are readily available.

Recent advances in Geographic Information Systems (*GIS*) technology and linkage of numerous models with *GIS* (e.g., Wilson and Lorang, 1999; Moore et al., 1993; Doe et al., 1996; Saghafian, 1996; Srinivasan and Arnold, 1994; Vieux et al., 1996; Johnston and Srivastava, 1999) have created a potential to develop an environment for coordination of conservation efforts at different management levels. These advances facilitate evaluation of prevention practices based not only on the type of the prevention measure, but also on their location within the watershed. Spatial analysis and simulation can also provide supporting information for allocation of resources to those areas and those types of practices which will provide the most effective protection.

To reflect the need for modeling at different levels of complexity, from fast, approximate estimates for risk assessment to more detailed simulations for predictions and land use design, a set of models with increas-

ing complexity was developed (Mitas and Mitasova, 1998; Mitasova et al., 1999). The simple models *RUSLE3D* (Revised Universal Soil Loss Equation for Complex Terrain) and *USPED* (Unit Stream Power-based Erosion Deposition) are based on modifications of well established equations representing special cases of erosion regimes. The basic empirical parameters for these models are available, however their applicability to a wide range of conditions is limited. The new distributed, process-based model *SIMWE* (SIMulated Water Erosion) provides capabilities to simulate more complex effects, however both the experimental and theoretical research are still very active and underlying equations, as well as the input parameters, are under continuing development.

This chapter presents theoretical basis for the distributed, process-based *SIMWE* model, describes the relation between the processes modeled by *SIMWE* and the *RUSLE3D* and *USPED* models and illustrates the use of the presented models for evaluation and design of different conservation measures.

2. METHODS

To model spatio-temporal distribution of sediment transport and erosion/deposition at any point and time, a complex system of interacting processes has to be simulated, including rainfall events, vegetation growth, surface, subsurface and ground water flow, soil detachment, transport and deposition. Excellent examples of continuous time simulation systems, which integrate a wide range of interacting processes important for land use management are *WEPP* (Flanagan et al., this volume), *LISEM* (Jetten and de Roo, this volume) or *SWAT* (Srinivasan and Arnold, 1994). Spatial components of these systems are usually based on 1D routing of water and sediment through homogeneous hydrologic units (e.g., hillslope segments, subwatersheds), limiting the range of spatial effects that can be simulated. To more accurately capture the impacts of spatially variable conditions a new generation of hydrologic and sediment transport models introduced 2D flow routing capabilities (*SIBERIA*: Willgoose and Gyasi-Agyei, 1995; *CASC2d*: Julien et al., 1995; Ogden and Heilig, this volume; *CHILD*: Tucker et al., this volume; *SIMWE*: Mitas and Mitasova, 1998). *SIMWE* uses spatially continuous approach to modeling of erosion and deposition with the modeled phenomena represented by *multivariate functions* and the flow of water and sediment described as *multivariate vector fields* rather than systems of 1D flows. The model was developed for subsystems describing overland water and sediment flow with focus on simulations of phenomena impor-

tant for land use management. The concept can be extended to other processes, including the 3D subsurface flows.

2.1 Process-based Overland Water and Sediment Flow Model

The spatially continuous approach uses a bivariate form of continuity equations to describe water flow and sediment transport over a complex terrain with spatially variable rainfall excess, land cover and soil properties during a rainfall event.

2.1.1 Shallow overland flow.

Shallow overland water flow is described by the bivariate form of the St Venant equations (e.g., Julien et al., 1995). The continuity relation is given by:

$$\frac{\partial h(\mathbf{r},t)}{\partial t} = i_e(\mathbf{r},t) - \nabla \cdot \mathbf{q}(\mathbf{r},t) \tag{1}$$

while the momentum conservation in the diffusive wave approximation has the form:

$$\mathbf{s_f}(\mathbf{r},t) = \mathbf{s}(\mathbf{r}) - \nabla h(\mathbf{r},t) \tag{2}$$

where $\mathbf{r} = (x, y)$ in m is the position, t in s is the time, $h(\mathbf{r}, t)$ in m is the depth of overland flow, $i_e(\mathbf{r}, t)$ in m/s is the rainfall excess = rainfall − infiltration, $\mathbf{q}(\mathbf{r}, t)$ in m^2/s is the unit flow discharge (water flow per unit width), $\mathbf{s}(\mathbf{r}) = -\nabla z(\mathbf{r})$ is the negative elevation gradient, $z(\mathbf{r})$ in m is the elevation, and $\mathbf{s_f}(\mathbf{r}, t)$ is the negative gradient of overland flow surface (friction slope).

For a shallow water overland flow, with the hydraulic radius approximated by the normal flow depth $h(\mathbf{r}, t)$ (Moore and Foster, 1990), the unit discharge is given by:

$$\mathbf{q}(\mathbf{r},t) = \mathbf{v}(\mathbf{r},t)h(\mathbf{r},t) \tag{3}$$

where $\mathbf{v}(\mathbf{r}, t)$ in m/s is the flow velocity. The system of equations (1-3) is closed using the Manning's relation between $h(\mathbf{r}, t)$ and $\mathbf{v}(\mathbf{r}, t)$

$$\mathbf{v}(\mathbf{r},t) = \frac{C}{n(\mathbf{r})} h(\mathbf{r},t)^{2/3} |\mathbf{s_f}(\mathbf{r})|^{1/2} \mathbf{s_{f0}}(\mathbf{r}) \tag{4}$$

where $n(\mathbf{r})$ is the dimensionless Manning's coefficient, $C = 1$ is the corresponding dimension constant in $m^{1/3}/s$ (Dingman, 1984), and $\mathbf{s_{f0}}(\mathbf{r}) =$

$\mathbf{s_f}(\mathbf{r})/|\mathbf{s_f}(\mathbf{r})|$ is the unit vector in the friction slope direction. To account for spatially variable cover necessary for land use management, we consider $n(\mathbf{r})$ as explicitly location dependent.

In this chapter, the solution of continuity and momentum equations for a steady state $\partial h(\mathbf{r},t)/\partial t = 0$, is considered to be an adequate estimate of overland flow for the land management applications (Flanagan and Nearing, 1995). In addition, the flow is considered to be close to the kinematic wave approximation for which $\mathbf{s_f}(\mathbf{r},t) \approx \mathbf{s}(\mathbf{r})$ and after using Equation (3), the Equation (1) is given by:

$$\nabla \cdot [h(\mathbf{r})\mathbf{v}(\mathbf{r})] = i_e(\mathbf{r}) \tag{5}$$

In order to incorporate the diffusive wave effects at least in an approximate way, Mitas and Mitasova (1998) incorporate a diffusion-like term $\propto \nabla^2[h^{5/3}(\mathbf{r})]$ into Equation (5):

$$-\frac{\varepsilon(\mathbf{r})}{2}\nabla^2[h^{5/3}(\mathbf{r})] + \nabla \cdot [h(\mathbf{r})\mathbf{v}(\mathbf{r})] = i_e(\mathbf{r}) \tag{6}$$

where $\varepsilon(\mathbf{r})$ is a spatially variable diffusion coefficient. Such an incorporation of diffusion in the water flow simulation is not new and a similar term has been obtained in derivations of diffusion-advection equations for overland flow, e.g., by Dingman, (1984) and Lettenmeier and Wood, (1992). The diffusion term, which depends on $h^{5/3}(\mathbf{r})$ instead of $h(\mathbf{r})$, makes Equation (6) *linear* in the function $h^{5/3}(\mathbf{r})$ which enables it to be solved using the path sampling method.

2.1.2 Erosion and sediment transport by overland flow.

The basic relationship describing sediment transport by overland flow is the sediment continuity equation, which relates the change in sediment storage over time, and the change in sediment flow rate along the hillslope to effective sources and sinks (e.g., Haan et al., 1994; Govindaraju and Kavvas, 1991; Foster and Meyer, 1972; Bennet, 1974). The bivariate form of the continuity of sediment mass equation is (e.g., Hong and Mostaghimi, 1995):

$$\frac{\partial[\rho_s c(\mathbf{r},t)h(\mathbf{r},t)]}{\partial t} + \nabla \cdot \mathbf{q_s}(\mathbf{r},t) = \text{sources} - \text{sinks} = D(\mathbf{r},t) \tag{7}$$

where $\mathbf{q_s}(\mathbf{r},t)$ in $kg/(ms)$ is the sediment flow rate per unit width, $c(\mathbf{r},t)$ in $particle/m^3$ is sediment concentration, ρ_s in $kg/particle$ is mass per sediment particle, $\rho_s c(\mathbf{r},t)$ in kg/m^3 is sediment mass density, and $D(\mathbf{r},t)$ in $kg/(m^2 s)$ is the net erosion or deposition rate. The sediment flow rate $\mathbf{q_s}(\mathbf{r},t)$ is a function of water flow and sediment concentration:

$$\mathbf{q_s}(\mathbf{r},t) = \rho_s c(\mathbf{r},t)\mathbf{q}(\mathbf{r},t) \tag{8}$$

Again, we assume a steady state form of the continuity equation:

$$\frac{\partial[\rho_s c(\mathbf{r},t)h(\mathbf{r},t)]}{\partial t} = 0 \quad \longrightarrow \quad \nabla \cdot \mathbf{q_s}(\mathbf{r}) = D(\mathbf{r}). \tag{9}$$

The sources and sinks term is derived from the assumption that the detachment and deposition rates are proportional to the difference between the sediment transport capacity and the actual sediment flow rate (Foster and Meyer, 1972):

$$D(\mathbf{r}) = \sigma(\mathbf{r})[T(\mathbf{r}) - |\mathbf{q_s}(\mathbf{r})|] \tag{10}$$

where $T(\mathbf{r})$ in $kg/(ms)$ is the sediment transport capacity, $\sigma(\mathbf{r})$ in m^{-1} is the first order reaction term dependent on soil and cover properties. The expression for $\sigma(\mathbf{r}) = D_c(\mathbf{r})/T(\mathbf{r})$ is obtained from the following relationship (Foster and Meyer, 1972):

$$D(\mathbf{r})/D_c(\mathbf{r}) + |\mathbf{q_s}(\mathbf{r})|/T(\mathbf{r}) = 1 \tag{11}$$

which states that the ratio of the erosion rate to the detachment capacity $D_c(\mathbf{r})$ in $kg/(m^2 s)$ plus the ratio of the sediment flow to the sediment transport capacity is a conserved quantity (unity). To keep the model simple, $\sigma(\mathbf{r})$ is applied for both net erosion and deposition. Equation (11), proposed by Foster and Meyer (1972), is based on the observed relationship between soil detachment and transport described e.g., by Meyer and Wischmeier (1969). This concept is used in several erosion models including *WEPP* (Haan et al., 1994; Flanagan and Nearing, 1995). The qualitative arguments, experimental observations and values for $\sigma(\mathbf{r})$ are discussed by Foster and Meyer, (1972) and Foster (1982). While it is possible to use other frameworks for estimation of $\sigma(\mathbf{r})$, we have chosen the Foster and Meyer concept because of its simplicity and widespread use.

The sediment transport capacity $T(\mathbf{r})$ and detachment capacity $D_c(\mathbf{r})$ represent the maximum potential sediment flow rate and the maximum potential detachment rate, respectively, and there are numerous simplified equations representing these rates under different conditions. In the *WEPP* model they are expressed as functions of a shear stress (Foster and Meyer, 1972):

$$T(\mathbf{r}) = K_t(\mathbf{r})[\tau(\mathbf{r})]^p \tag{12}$$

$$D_c(\mathbf{r}) = K_d(\mathbf{r})[\tau(\mathbf{r}) - \tau_{cr}(\mathbf{r})]^q \tag{13}$$

where $\tau(\mathbf{r}) = \rho_w\, g h(\mathbf{r}) \sin\beta(\mathbf{r})$ in Pa is the shear stress, β in deg is the slope angle, p and q are exponents, $K_t(\mathbf{r})$ in s is the effective transport

capacity coefficient, $K_d(\mathbf{r})$ in s/m is the effective erodibility (detachment capacity coefficient), $\rho_w\, g$ is the hydrostatic pressure of water with the unit height, $g = 9.81$ in m/s^2 is the gravitational acceleration, $\rho_w = 10^3$ in kg/m^3 is the mass density of water, and $\tau_{cr}(\mathbf{r})$ in Pa is the critical shear stress. The parameters and adjustment factors for the estimation of $D_c(\mathbf{r})$ in $T(\mathbf{r})$ are functions of soil and cover properties, and their values for a wide range of soils, cover, agricultural and erosion prevention practices were developed within the *WEPP* model (Flanagan and Nearing, 1995).

The exponents p, q substantially influence model behavior. The *WEPP* model uses $q = 1$ and $p = 1.5$ which means that with increasing water flow, transport capacity increases faster than detachment. The comparison with the spatial extent of colluvial deposits in our previous study (Mitas and Mitasova, 1998) indicates that over long term period (decades) the pattern of erosion/deposition is closer to the results obtained with a lower value of p. This is in agreement with several studies which indicate that for the landscape scale modeling the Equations (12) and (13) are not general enough for different types of flow and sediment transport processes present in complex landscapes (Willgoose et al., 1989; Kirkby, 1987; Willgoose and Gyasi-Agyei, 1995; Mitas and Mitasova, 1998).

Similar to the water flow equation, the steady state sediment flow equation (Equation 9) can be rewritten to include a diffusion term. First, a function representing the mass of water-carried sediment per unit area $\varrho(\mathbf{r})$ in kg/m^2 is defined as:

$$\varrho(\mathbf{r}) = \rho_s c(\mathbf{r}) h(\mathbf{r}) \tag{14}$$

and after introducing a small diffusion term $\propto \nabla^2 \varrho(\mathbf{r})$, the continuity equation is rewritten as:

$$-\frac{\omega}{2}\nabla^2 \varrho(\mathbf{r}) + \nabla \cdot [\varrho(\mathbf{r})\mathbf{v}(\mathbf{r})] + \varrho(\mathbf{r})\sigma(\mathbf{r})|\mathbf{v}(\mathbf{r})| = \sigma(\mathbf{r})T(\mathbf{r}) \tag{15}$$

where ω in m^2/s is the diffusion constant. On the left hand side of Equation (15) the first term describes local diffusion, the second term is a drift driven by the water flow while the third term represents a velocity dependent 'potential' acting on $\varrho(\mathbf{r})$. The size of the diffusion constant is about one order of magnitude smaller than the reciprocal Manning's constant so that the impact of the diffusion term is relatively small. It represents local dispersion processes of the suspended flow (Bennet, 1974), caused by microtopography which is not captured by the *DEM*. The diffusion term can be modified to reflect impact of various processes.

The water and sediment flow described by Equations (6) and (15) can be solved by the path sampling stochastic approach described in the following section.

2.2 Path Sampling Solution Method

Equations (6) and (15) have a similar form in which a linear differential operator $\mathcal{O}$ acts on a nonnegative unknown function $\gamma(\mathbf{r})$ (either $h(\mathbf{r})$ or $\varrho(\mathbf{r})$), while on the right hand side, there is a given source term $\mathcal{S}(\mathbf{r})$ (either $i_e(\mathbf{r})$ or $\sigma(\mathbf{r})T(\mathbf{r})$):

$$\mathcal{O}\gamma(\mathbf{r}) = \mathcal{S}(\mathbf{r}) \tag{16}$$

Denoting $\mathcal{O}^{-1}$ the inverse operator to $\mathcal{O}$, the solution can be symbolically written as:

$$\gamma(\mathbf{r}) = \mathcal{O}^{-1}\mathcal{S}(\mathbf{r}) \tag{17}$$

or explicitly, using the Green's function:

$$\gamma(\mathbf{r}) = \int_0^\infty \int G(\mathbf{r}, \mathbf{r}', p)\mathcal{S}(\mathbf{r}')d\mathbf{r}'dp \tag{18}$$

The Green's functions are often used for expressing the solutions of linear differential equations in physical or mathematical applications. For the theory see, e.g., Karlin and Taylor, (1981); Glimm and Jaffe, (1972); Stakgold, (1979); Carslaw and Jaeger, (1947). $G(\mathbf{r}, \mathbf{r}', p)$ is given by the following equation and an initial condition:

$$\frac{\partial G(\mathbf{r}, \mathbf{r}', p)}{\partial p} = -\mathcal{O}G(\mathbf{r}, \mathbf{r}', p)\,; \;\; G(\mathbf{r}, \mathbf{r}', 0) = \delta(\mathbf{r} - \mathbf{r}') \tag{19}$$

where $\mathbf{r}, \mathbf{r}'$ are locations, p is time and δ is the Dirac function. In addition, we assume that the spatial region is a delineated watershed with zero boundary condition which is fulfilled by $G(\mathbf{r}, \mathbf{r}', p)$. The corresponding equations can be solved, e.g., by projection methods (Rouhi and Wright, 1995). Another equivalent alternative is to interpret Equations (6),(15) and (16) as describing stochastic processes with diffusion and drift components (Fokker-Planck equations) and carry out the actual simulation of the underlying process using a path sampling method (Gardiner, 1985).

The method is based on duality between the particle and field representation of spatially distributed phenomena.Within this concept, density of particles in space defines a field and vice versa, field is represented

by particles with corresponding spatial distribution of their densities. Using this duality, processes can be modeled as evolution of fields or evolution of spatially distributed particles (Figure 1), with the solution obtained as follows.

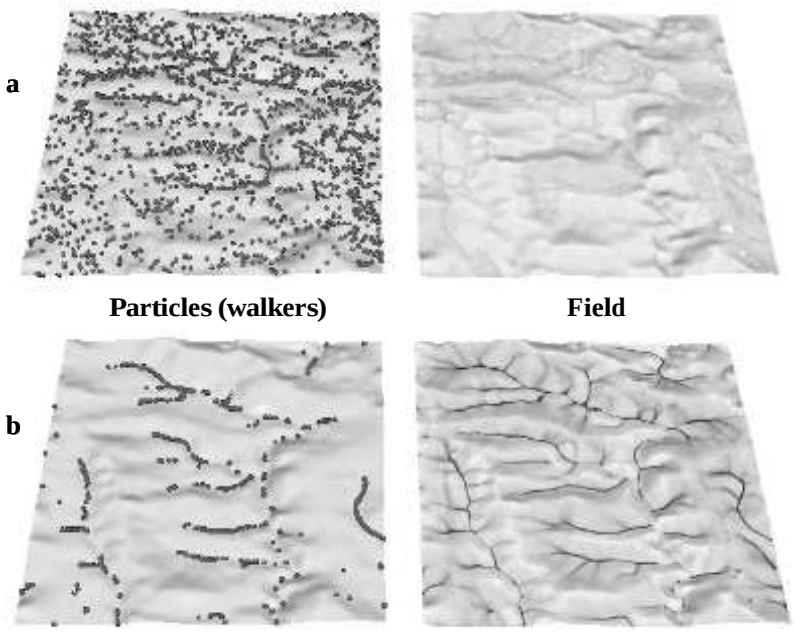

Figure 1. Path sampling solution of the continuity equation for water depth $h(\mathbf{r})$ using duality between particle and field representation: a) water depth at 1 minute, b) water depth after 24 minutes. The grid is 416x430 cells at 10m resolution. See the *CDROM* for animation.

First a selected number of particles, also called walkers or sampling points, is distributed according to the source $\mathcal{S}(\mathbf{r}')$. These walkers are then propagated according to the function $G(\mathbf{r}, \mathbf{r}', p)$, generating a number of sampling paths. Averaging of these path samples provides an estimation of the actual solution $\gamma(\mathbf{r})$ with statistical accuracy proportional to $1/\sqrt{M}$ where M is the number of walkers (Figure 2). The solution is not restricted to the steady state and the state of the modeled quantity at any given time p can be obtained by averaging the path samples at a given time p.

The path sampling technique has several unique advantages which are becoming even more important due to new developments in computer technology. Perhaps one of its most significant properties is robustness

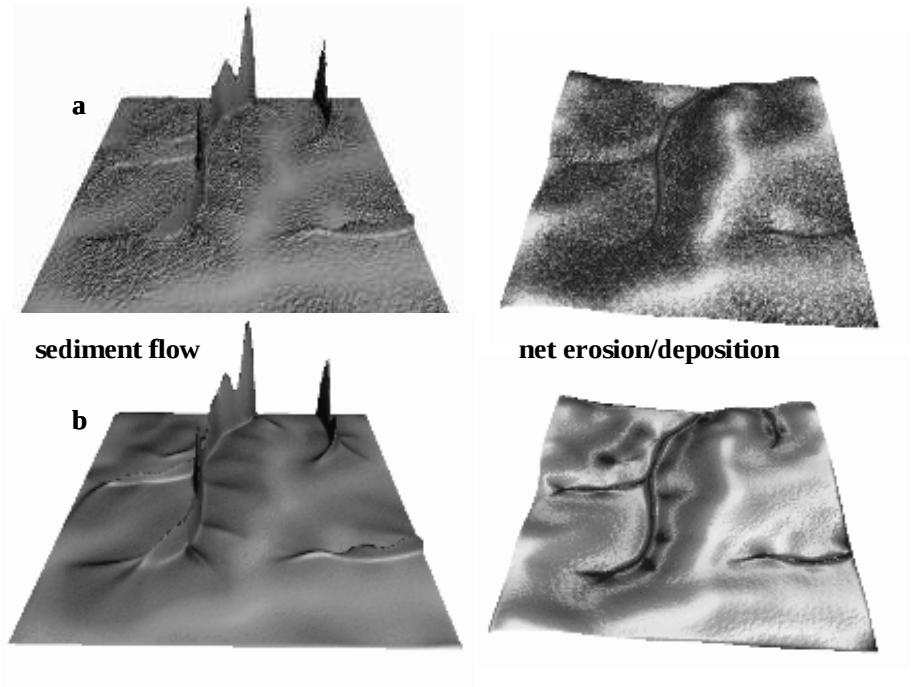

Figure 2. Path sampling solution of the continuity equation for sediment flow and net erosion/deposition: a) results for 7000 walkers, b) results for 50 million walkers. The grid is 280x250(70,000 cells) at 2m resolution. See the *CDROM* for animation.

which makes it possible to solve the equations for complex cases, such as discontinuities in the coefficients of differential operators (in our case, abrupt slope or cover changes, etc). In addition, the independence of sampling points makes the stochastic methods perfectly suited to the new generation of computers as they provide scalability from a single workstation to large parallel machines and computers distributed over different types of networks.

3. SIMPLIFIED SPECIAL CASES AND MODEL EXTENSIONS

Land use management poses specific challenges for hydrologic and erosion simulations because of the necessity to capture the spatial aspects of the modeled processes. In the following sections some of the issues important from the point of view of landuse design are addressed, in particular the simplified erosion and deposition models, simulation of

water flow in flat areas and depressions, and modeling with spatially variable resolution.

3.1 Simple Erosion and Deposition Models

To satisfy the need for models which are easy to implement, simple to compute, and for which the data a readily available, it is useful to derive the models for special cases of sediment transport regimes. There are two limiting cases of erosion and sediment transport (Foster and Meyer, 1972; Hairsine and Rose, 1992; Tucker et al., this volume): (i) *detachment limited*, and (ii) *sediment transport capacity limited*.

3.1.1 The detachment limited case.

This case is represented by $\sigma \rightarrow 0$, which, after substituting into Equations (9)-(10) results in the net erosion equal to the detachment capacity $D(\mathbf{r}) = D_c(\mathbf{r})$. It can be directly computed from Equation (13) using an estimate of water depth $h(\mathbf{r})$ computed, for example, by the *SIMWE* water flow module. For this case, transport capacity exceeds detachment capacity everywhere, erosion and sediment transport is detachment capacity limited and therefore no deposition occurs.

The most common erosion model which represents this case is *USLE* and its revised version *RUSLE* (Lane et al., this volume). If we assume that $\tau_{cr}(\mathbf{r}) = 0$ and that the spatial distribution of steady state water flow is adequately represented by a function of upslope contributing area per unit width (e.g., Moore et al., 1993) the detachment limited erosion can be approximated by *RUSLE3D*, which for a point on a hillslope has the form (Moore et al., 1993; Mitasova et al., 1999; see also Desmet and Govers, 1996 for hillslope segment based equation):

$$D(\mathbf{r}) = R(\mathbf{r})K(\mathbf{r})C(\mathbf{r})P(\mathbf{r})(m+1)[A(\mathbf{r})/22.13]^m[sin\beta(\mathbf{r})/0.09]^n \quad (20)$$

where $D(\mathbf{r})$ in $ton/(acre.year) = 0.2242kg/(m^2.year)$ is the average annual soil detachment (soil loss) rate, $A(\mathbf{r})$ in m^2/m is the upslope contributing area per unit width, $22.13m$ is the length and 0.09 is the slope of the standard USLE plot, $R(\mathbf{r})$ in $(hundreds\,of\,ft{-}tonf.in)/(acre.hr.year)$ $= 17.02\ MJ.mm/(ha.hr.year)$ is the rainfall energy factor, $K(\mathbf{r})$ in $ton.acre.hr/(hundreds\,of\,acre ft{-}tonf.in) = 0.1317\,t.ha.hr/(ha.MJ.mm)$ is soil erodibility, $C(\mathbf{r})$ [dimensionless] is the cover factor and $P(\mathbf{r})$ [dimensionless] is the prevention measures factor (Haan et al., 1994; Lane et al., this volume). Single storm and monthly $R(\mathbf{r})$ is also available, making Equation (20) suitable for estimation of $D(\mathbf{r})$ for single storms and

for modeling of monthly soil loss distribution over a year (Haan et al., 1994). Exponents m, n depend on the prevailing type of erosion (sheet, rill) and the typical values are $m = 0.4 - 0.6$ and $n = 1 - 1.3$. Replacement of slope length used in the original formulation of *USLE/RUSLE* by the upslope area provides a better spatial description of increased erosion due to the concentrated flow without the need to *a priori* define these locations as inputs for the model.

3.1.2 Transport capacity limited erosion.

For this case $\sigma \to \infty$, which, after substituting into Equation (10), leads to $|\mathbf{q}_s(\mathbf{r})| \approx T(\mathbf{r})$ and net erosion/deposition can be computed directly as a divergence of the sediment transport capacity:

$$D(\mathbf{r}) = \nabla \cdot \mathbf{q}_s(\mathbf{r}) = \nabla \cdot [T(\mathbf{r})\mathbf{s_0}(\mathbf{r})] \tag{21}$$

where $\mathbf{s_0}(\mathbf{r}) = \mathbf{s}(\mathbf{r})/|\mathbf{s}(\mathbf{r})|$ is the unit vector in the steepest slope direction. Mitas and Mitasova (1998) have shown that the results obtained for this case were close to the observed distribution of colluvial deposits in their study area, suggesting the prevailing influence of the transport capacity limited case on a long term pattern of deposition. Equation (21) was also used to demonstrate the impact of both tangential and profile curvatures and the importance of 2D flow routing for predicting net erosion/deposition pattern (Mitas and Mitasova, 1998).

The Unit Stream Power Based Erosion/Deposition model (*USPED*) estimates the transport capacity limited case of erosion/deposition using the idea originally proposed by Moore and Burch (1986). It combines the *USLE/RUSLE* parameters and upslope contributing area per unit width $A(\mathbf{r})$ to estimate the sediment flow at sediment transport capacity:

$$q_s(\mathbf{r}) = T(\mathbf{r}) \approx R(\mathbf{r})K(\mathbf{r})C(\mathbf{r})P(\mathbf{r})[A(\mathbf{r})]^m[sin\beta(\mathbf{r})]^n \tag{22}$$

The net erosion/deposition $D(\mathbf{r})$ is then estimated using Equation (21) as:

$$D(\mathbf{r}) = \nabla \cdot [T(\mathbf{r})\mathbf{s_0}(\mathbf{r})] = \frac{d[T(\mathbf{r})cos\alpha(\mathbf{r})]}{dx} + \frac{d[T(\mathbf{r})sin\alpha(\mathbf{r}))}{dy} \tag{23}$$

where $\alpha(\mathbf{r})$ in *deg* is the aspect of the terrain surface (direction of flow). The exponents m, n control the relative influence of water and slope terms and reflect the impact of different types of flow. The exponents leading to values of erosion rates on hillslopes consistent with the values from *RUSLE* are $m = 1.6, n = 1.3$ and they seem to reflect the pattern for prevailing rill erosion with erosion sharply increasing with the amount of water. The observed extent of colluvial deposits in our previous study

(Mitas and Mitasova, 1998) indicated that a lower exponent $m = 1$ better reflects the pattern of compounded, long term impact of both rill and sheet erosion and averaging over a long term sequence of large and small events.

Models representing limiting cases of erosion are simple to compute in GIS by combining the flow-tracing and topographic analysis functions with map algebra. They can be applied to a single storm, monthly and annual estimates of soil detachment and net erosion/deposition. Caution should be used when interpreting the results from both *RUSLE3D and USPED* because the *USLE/RUSLE* parameters were developed for simple plane fields and detachment limited erosion. Therefore, to obtain accurate quantitative predictions for complex terrain and land cover conditions they need to be re-calibrated, especially in areas of concentrated flow (Foster, 1990; Mitasova et al., 1997 reply). While the capabilities of both *RUSLE3D and USPED* to accurately predict the rates of erosion and deposition at any point in the complex landscape are limited (fact which is true about almost any erosion model), they are useful tools for land management. Both models use readily available parameters and can provide valuable spatial information about: (i) the location of areas with high erosion risk from both shallow overland and concentrated flow, (ii) location of areas with deposition, and (iii) relative estimates of erosion and deposition rates for different land use alternatives and conservation strategies. Locations identified as high risk from both *RUSLE3D and USPED* should be primary targets for field erosion inventory (to validate the risk) and implementation of prevention/mitigation measures (if the high risk is confirmed in the field). Computation of net erosion and deposition is also useful for evaluation of the landscape's capacity to deposit the eroded material before it can reach the streams.

3.2 Water Depth in Flat Areas and Depressions

While flat areas and depressions are not high erosion risk locations, they play an important role within watersheds by holding water and reducing water flow to neighboring steeper slopes or into the streams. Modeling water flow over terrain surfaces with $\nabla z > 0$ can be successfully performed using kinematic wave approximation. However, flat areas and bottoms of depressions where $\nabla z \to 0$ pose a problem because the water flow direction becomes undefined. Incorporation of the spatially variable diffusion term $\varepsilon(\mathbf{r})$ in the SIMWE model provides capabilities to approximately simulate water depth in these locations. By defining the diffusion term $\varepsilon(\mathbf{r})$ as a function of water depth and the

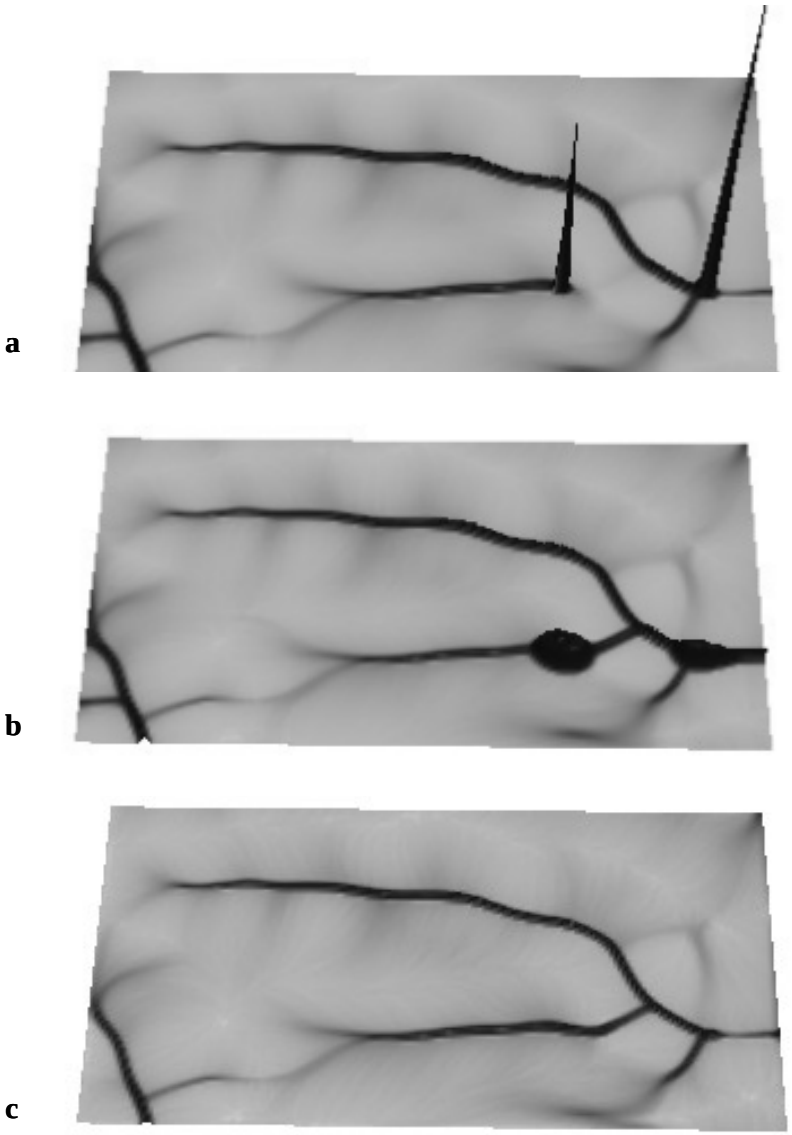

Figure 3. Simulation of water flow through existing shallow depressions: a) 2D kinematic wave flow, b) approximate 2D diffusive wave flow with variable $\varepsilon(\mathbf{r})$ and flow momentum, c) approximate 2D diffusive wave flow with a shallow, 1 degree slope channel running through the depressions. Simulation was performed by the *SIMWE* model using a 10m resolution *DEM*, 100x170 cells. See the *CDROM* for animation.

velocity of flow as a function of an approximate water flow momentum, the water fills the depressions or spreads in the flat area and flows out in the prevailing flow direction (Figure 3b).

For the situations when the flat areas or depressions are drained by natural or man-made swales and channels, the water flow can be simulated by combining the gradient field derived from the *DEM* with the gradient of the drainage (Figure 3c). The input vector field $\mathbf{s}(\mathbf{r})$ representing the flow direction is then defined as:

$$\mathbf{s}(\mathbf{r}) = (1 - \delta_{ij})\mathbf{s_e}(\mathbf{r}) + \delta_{ij}\mathbf{s_d}(\mathbf{r}) \tag{24}$$

where $\mathbf{s_e}(\mathbf{r})$ is the vector in the steepest slope direction derived from a *DEM* and $\mathbf{s_d}(\mathbf{r})$ is the vector representing the flow through the surface drainage which can be estimated, for example, from drainage line data using GIS tools and/or from field measurements.

3.3 Multiscale Water and Sediment Flow Simulation

Because the spatial unit modeled at the site level is part of a larger watershed, the evaluation of the impact of numerous, locally implemented conservation practices across the entire watershed requires multiscale approach. This approach links the high resolution, local level simulation with low resolution/regional simulation and is being implemented for the *SIMWE* model. It supports simulations with spatially variable resolution which can include the following cases: (i) study area is represented by several data sets with different resolutions and levels of accuracy, and the best available data are used for each subregion; (ii) study area is large, with spatially variable complexity and it is sufficient to run the more homogeneous areas at lower resolution while running the more complex areas or areas experiencing land use change at high resolution. Both *spatially variable accuracy* and *resolution* can be implemented by reformulating the solution through the Green's function given by Equation (18). The integral Equation (18) can be multiplied by a *reweighting* function $W(\mathbf{r})$:

$$W(\mathbf{r})\gamma(\mathbf{r}) = \int_0^\infty \int W(\mathbf{r})G(\mathbf{r}, \mathbf{r}', p)\mathcal{S}(\mathbf{r}')d\mathbf{r}'dp = \tag{25}$$

$$= \int_0^\infty \int G^*(\mathbf{r}, \mathbf{r}', p)\mathcal{S}(\mathbf{r}')d\mathbf{r}'dp \tag{26}$$

which is equal to the appropriate increase in accuracy ($W(\mathbf{r}) > 1$) in the

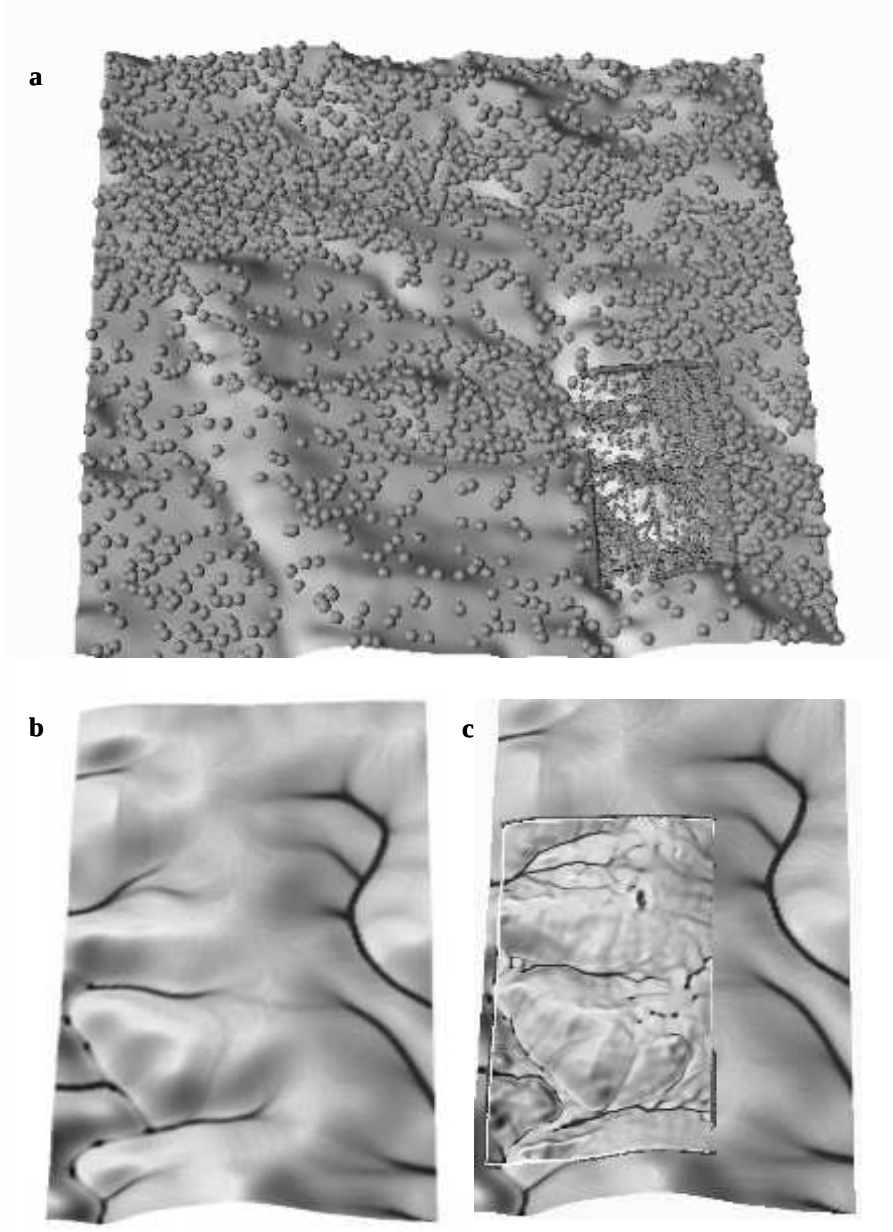

Figure 4. Simulation of water depth at spatially variable resolution 10m and 2m: a) initial particle representation, b) detail of resulting water depth at 10m resolution c) detail at 2m resolution. See the *CDROM* for animation

regions of interest while it is unity elsewhere. The function $W(\mathbf{r})$ can change (abruptly or smoothly) between regions with unequal resolutions and in fact, can be optimally adapted to the quality of input data (terrain, soils, etc) so that the more accurate solution is calculated only in the regions with correspondingly accurate inputs.

The reweighted Green's function $G^*(\mathbf{r}, \mathbf{r}', p)$, in effect, introduces a higher density of sampling points in the region with large $W(\mathbf{r})$. The statistical noise will be spatially variable as $\approx 1/[W(\mathbf{r})\sqrt{M}]$, where M is the average number of samples resulting in the accuracy increase for the areas with $W(\mathbf{r}) > 1$.

This approach provides an alternative to the finite element methods (see e.g. Tucker et al., this volume) because it uses multiple standard grids with the given resolutions instead of finite element meshes, which often lack adequate *GIS* support. The implementation is based on the multipass simulation. First, the entire area is simulated at lower resolution, and the walkers entering the high resolution area(s) are saved. The saved walkers are resampled according to the Equation (25) by spliting each walker into a number of "smaller" walkers which are randomly distributed in the neighborhood of the original walker. The model is then run at high resolution only for the given subarea, with the resampled walkers used as inputs (Figure 4). If several different land use alternatives are considered for the given subarea, this approach can be used to perform simulations for each alternative only within the high resolution subarea. The approach also provides useful spatial information about the locations where water flows into the given subarea and where it flows out (Figure 4c).

4. LANDSCAPE SCALE EROSION PREVENTION PLANNING AND DESIGN

Interactions between different land covers and topography significantly influence the spatial distribution of surface water depth, sediment flow and net erosion/deposition. The capabilities to simulate these interactions at both watershed and field scale can support the design of sustainable, cost effective conservation strategies and erosion prevention measures. Mitasova and Mitas (1998) have demonstrated the use of *SIMWE* and *GIS* for finding an effective spatial distribution of protective grass cover for a small agricultural watershed. The following sections provide examples of a wide range of applications where simulations of water flow, sediment transport and erosion/deposition are used to support land use management at different scales and levels of complexity.

4.1 Watershed Scale Erosion Risk Assesment and Evaluation of Conservation Strategies with Simple Distributed Models

A large number of watershed associations are being organized (*EPA*, 2000) with the goal of improving the management of America's watersheds. The basis for this work are watershed management plans which identify the problems and set priorities in funding and implementation of conservation measures. *GIS* combined with simple erosion models and free spatial data available through the National Spatial Data Clearinghouse (*NSDI*, 2000) provide a cost effective way to assess the current state of watersheds, as well as evaluate the impact and prioritize various conservation strategies. The simplified models *RUSLE3D and USPED* were applied to the Court Creek watershed which serves as a pilot area for the Illinois Department of Natural Resources (*IDNR*) program aimed at demonstration of community based watershed management with strong scientific support. First, the current erosion risk areas were identified and their pattern was analyzed using *RUSLE3D* and *GIS* tools (Figure 5b). The analysis shows a favorable land use pattern with protective forested buffers along the bigger streams and on steep slopes. However, the analysis also indicates that headwater areas and areas with lower values of slope and convergent water flow are not sufficiently protected. These sensitive areas are relatively small and scattered, and the results from *RUSLE3D* indicate that only 16 percent area (10,000 acres) produces 87 percent of total detached soil available for transport.

The impact of several conservation strategies was then evaluated, with the following two alternatives presented here: (i) 30m protective buffers along the bigger streams with rest of the watershed in agriculture; (ii) critical area planting of conservation areas based on the erosion risk map. The comparison of the strategies in terms of gain or loss of agricultural land and reduction of erosion for a high risk Court Creek subwatershed is presented in Figure 5. The analysis demonstrates that a 30m buffer along the main stream does not provide adequate erosion protection. While it would make 94 percent of the area available to agriculture, it would also lead to a three fold increase in average annual soil loss. Elimination of high erosion potential would require reduction of agricultural land by only 5 percent and extension of the criteria currently used for the conservation program by including the headwater areas and areas with convergent water flow.

The results obtained from the *USPED* model indicate that a substantial portion of the eroded soil moves only for a short distance and there is enough concave areas to deposit the sediment before it can enter the

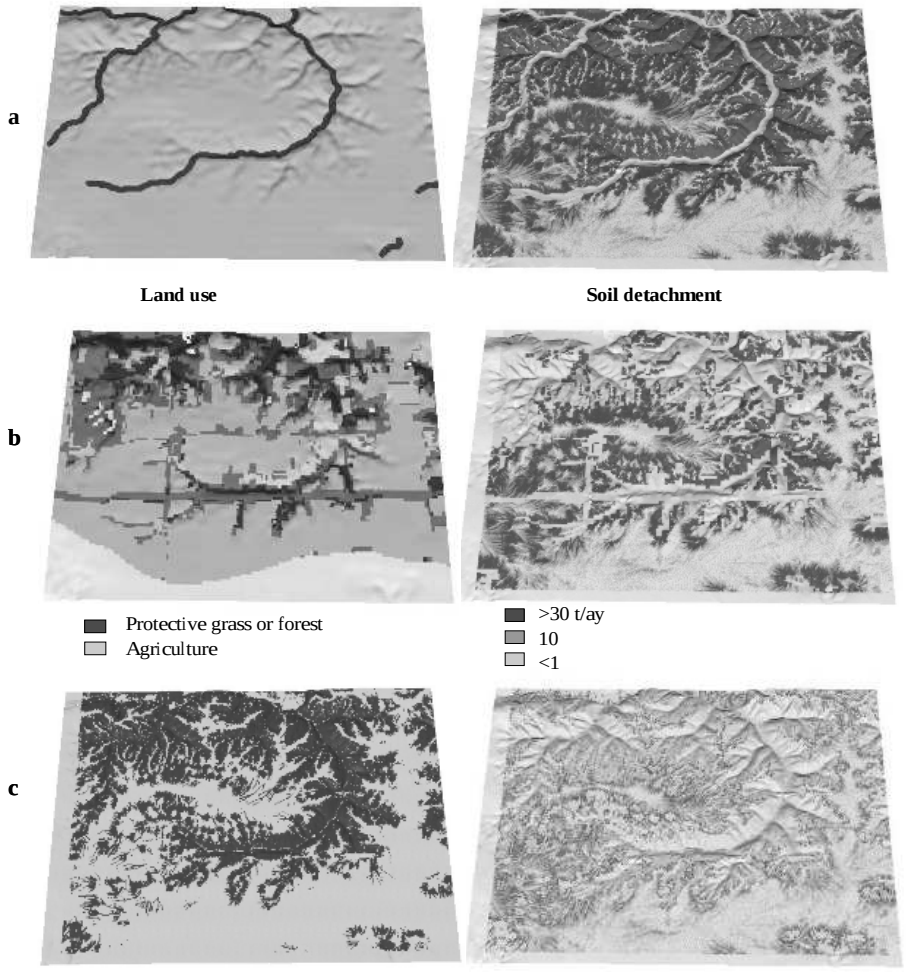

Figure 5. Court Creek subwatershed soil detachment for different land use alternatives estimated by *RUSLE3D*: a) 30m buffers along the streams, 94 percent row crops, soil loss 27t/(ac.yr), b) current land use, 63 percent row crops/grains, soil loss 8t/(ac.yr), c) grass cover in areas with soil detachment¿10 t/(acre.yr), 58 percent row crops, soil loss 1 t/(acre.yr). The area is 3.6x4.6km modeled at 10m resolution. (see also http://www2.gis.uiuc.edu:2280/modviz/courtcreek/cc.html)

streams.

These results support some recent observations and hypotheses (Roseboom and Mollahan, 1999; Trimble, 1999) that in the Midwestern watersheds most of the sediment observed in the streams originates within

the streams and from erosion by concentrated flow rather than from hillslope erosion by shallow overland flow.

This application demonstrates that the simple models used with widely available data can be useful for preliminary assessment of erosion and sedimentation risk, identification of "hot spots" in the watersheds and approximate evaluation of different conservation strategies.

4.2 Wetlands and Drainage

4.2.1 Topographic potential for wetlands.

Preservation and restoration of wetlands is among the most important and popular best management practices. Their success depends on many factors, including a sufficient supply of water. The *SIMWE* hydrologic submodel was used to identify the locations within the Court Creek Pilot Watershed which have topographic conditions favorable for

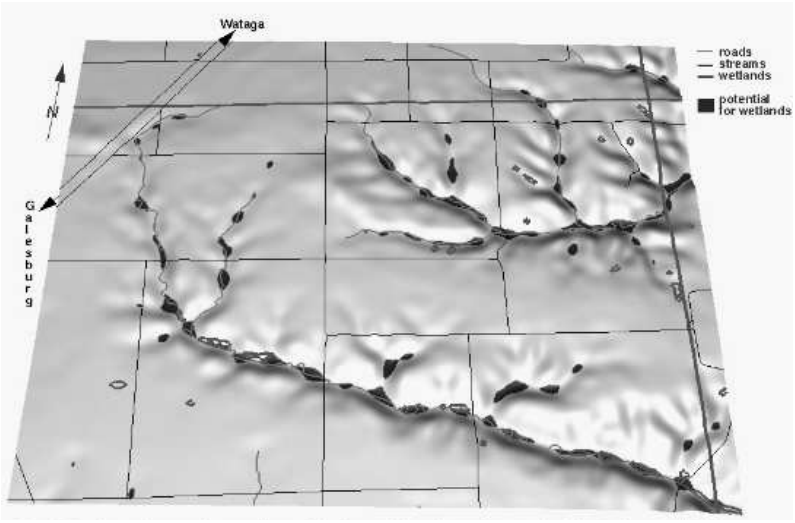

Figure 6. Map of topographic potential for wetlands. Existing wetlands are displayed as polygons and cover 1% of the subwatershed while the model identifies 6% area as suitable for wetlands. The area is 4x6km, simulated at 10m resolution (resampled from 30m resolution *DEM*)

.

wetlands. Several simulations were performed for various rainfall intensities, uniform land cover and saturated soil conditions, assuming that the flow velocity is controlled only by the terrain gradient - the existing

drainage and channels were not considered. Comparison of the simulated water depth with existing wetland areas shows that these areas are characterized by steady state water depth from one event of at least 0.3m. Using this threshold, a map for topographic potential for wetlands was computed using map algebra (Figure 6). While the simulation was very simplified, the map can serve as a useful starting point for identification of land owners with suitable land for wetlands and for evaluation of the proposals for wetland locations.

4.2.2 Drainage location design.

Simulation of spatial distribution of water depth provides valuable information also for an "opposite" task - identification of locations which require drainage to prevent negative impact of standing water on yields. Using a high accuracy *DEM* (6m resolution, 0.05m vertical accuracy) interpolated from rapid kinematic survey data by the *RST* method (Mitas and Mitasova, 1999), the water depth distribution was simulated for a typical rainfall for Midwestern agricultural fields (9mm/hr) under saturated conditions. The resulting water depth map was used to evaluate suitability of the locations of current drainage and to plan the location of new drainage network in the negatively affected field (Figure 7). While the model was very useful for evaluating and planning a suitable spatial pattern of the drainage network, detailed soil data and more complex dynamic simulations are needed to design the size, depth and other parameters of the drainage.

4.3 Concentrated Flow Erosion and Grassed Waterways

The suitability of the *SIMWE* model for spatial design of vegetation based best management practices was evaluated by application to small experimental watersheds with planned or installed erosion prevention measures.

4.3.1 Concentrated flow erosion.

Development of high erosion in areas of concentrated flow was studied by performing simulations of water flow and net erosion deposition for an experimental field with uniform land cover (350x270m, modeled at 2m resolution; Zhang, 1999). For a short rainfall event ending before the flow has reached steady state, the maximum erosion rate was on

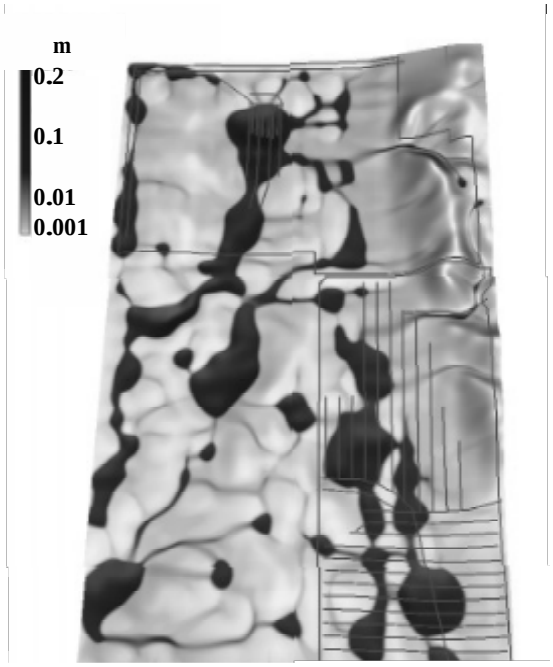

Figure 7. Simulated spatial distribution of water depth for agricultural fields (2.5x4.5km) draped as color over the *DEM* (6m resolution, 30-times vertical exaggeration), with the existing drainage drawn as lines.

the upper convex part of the hillslope and there was only deposition in the center of the valley (Figure 8a). As the duration of the rainfall increased, water depth in the center of the valley has grown rapidly until it reached a threshold when linear features with very high erosion rates developed within the depositional area, indicating potential for gully formation (Figure 8b). This effect is modeled by both USPED (Mitasova et al., 1996, 1999) and SIMWE (Mitas and Mitasova, 1998), however, a smooth, high resolution DEM without artifacts is needed to realistically capture this commonly observed phenomenon (see Figure 2c in Mitas and Mitasova, 1999). This example also demonstrates that for a dynamic event modeling incorporation of re-entrainment process is important and should be incorporated into the *SIMWE* model (Hairsine and Rose, 1992).

4.3.2 Grassed waterways.

The common practice for prevention of erosion by concentrated flow are grassed waterways. Their design is guided by the topographic con-

Figure 8. Water depth and net erosion/deposition pattern for 18mm/hr rainfall excess for a) short event, with only deposition in the valley center, b) long event leading to steady state flow, with both high erosion and deposition in the valley center, indicating a potential for gully formation. The 350x270m field is modeled at 2m resolution. See animation on *CDROM*.

ditions and roughness within the grassed area, represented by Mannings coefficient (*SCS*, 1988). To investigate the impact of a grassed waterway, the water and sediment flow as well as net erosion/deposition pattern were simulated for a field within the Scheyern experimental farm (Auerswald et al., 1996; Mitas and Mitasova, 1998) for the bare soil conditions and after the installation of grassed waterway with different values of roughness in the field. For the bare field, there is a potential for gully formation (Figure 9a). After the installation of grassed waterway the center of the valley becomes a depositional area. However, if the roughness in the field is several times smaller than in the grassed area, high erosion develops around the waterway, potentially replacing one big gully with two smaller ones. This "double channeling" problem can substantially increase the cost of the waterway maintenance (Figure 9b). Increasing the roughness in the field reduces the risk of double channeling and the transition from erosion in the field to deposition in the grassed area is relatively smooth (Figure 9c). An alternative solution

combines contour filter strip on the upper convex part of the hillslope with grassed waterway (Mitas and Mitasova, 1998).

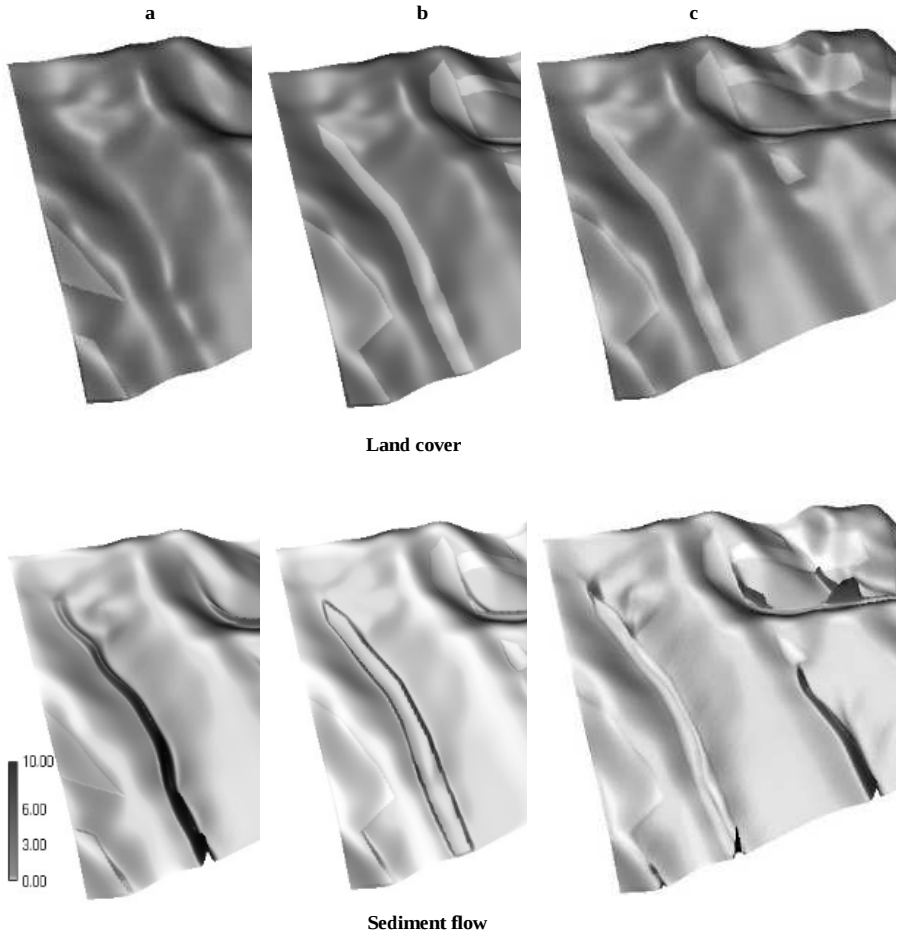

Figure 9. Impact of grassed waterway and differences in roughness on sediment flow: a) bare field with gully potential in the center, b) grassed waterway (light grey, n=0.1) and the bare field (dark grey, n=0.01) with sediment flow along the grassed waterway (double channeling), c) grassed waterway (n=0.1) and the field with increased roughness (n=0.05) without increase in sediment flow along the waterway and smooth transition from erosion to deposition. See erosion/deposition in color on *CDROM*.

5. CONCLUSIONS

This chapter is focused on methodology and applications of simulation methods for prediction and solution of land management problems related to overland flow erosion. The presented approach aims at keeping the models, and particularly the number of required input parameters, as simple as possible while capturing the effects important for sustainable land use design. The applications demonstrate the need for a set of modeling tools with different levels of complexity to support land use management from strategic planning to design and implementation. To satisfy this need three interrelated models were presented.

The first model *SIMWE* is based on generalization of hillslope erosion model used in *WEPP* (Flanagan and Nearing, 1995). It models erosion regimes from detachment to transport capacity limiting cases, includes approximate diffusive wave effect and it supports multiscale modeling which can be further extended to incorporate multiscale-multiprocess simulations.

RUSLE3D/USPED differ from *SIMWE* in that they model only the limited cases of erosion and sediment transport, however they use readily available parameters and therefore are easy to implement and use (see on-line tutorials for *GRASS5* and *ArcView* by Mitasova and Mitas, 1999a,b). All of the presented models can be used for single storms as well as for long term averages.

The applications of spatially continuous simulations revealed gaps in the theory of erosion processes in complex landscapes, especially in the mathematical description of transport capacity suitable for complex landscapes. Spatially distributed field experiments based on new technologies for field data collection, monitoring and remote sensing closely coupled with modeling are needed to improve our understanding of complex interactions involved in erosion processes and bring the quantitative accuracy of predictions (which is currently at about 50-150%) to acceptable and useful levels.

The report "New Strategies for America's Watersheds" (Committee on Watershed Management, National Research Council 1999) identifies simulation modeling as one area of special promise for watershed management. At the same time, this report analyzes the current status in watershed modeling for decision making and concludes that the available models and methods are outdated and "a major modeling effort is needed to develop and implement state-of-the-art models for watershed evaluations"(pp.160-161). The presented approach along with other models presented in several chapters in this book, are a step towards the development and implementation of such tools.

ACKNOWLEDGMENTS

We would like to acknowledge the long term support for this research from Geographic Modeling Systems Laboratory director Douglas M. Johnston as well as *GIS* assistance by William M. Brown. The funding was provided by the *USArmy CERL*, Strategic Environmental Research and Development Program - *SERDP*, Illinois Council on Food and Agricultural Research - *CFAR* and Illinois Department of Natural Resources. We greatly appreciate the sharing of data by K. Auerswald, S. Warren, K. Drackett, Zhang Yusheng, and D. Timlin. Our special thanks goes to two reviewers for their thorough review of the paper, as well as for their stimulating questions and comments which significantly helped to improve the revised version of this chapter.

REFERENCES

Auerswald, K., A. Eicher, J. Filser, A. Kammerer, M. Kainz, R. Rackwitz, J. Schulein, H. Wommer, S. Weigland, and K. Weinfurtner, 1996, Development and implementation of soil conservation strategies for sustainable land use - the Scheyern project of the FAM, in: *Development and Implementation of Soil Conservation Strategies for Sustainable Land Use*, edited by H. Stanjek, Int. Congress of ESSC, Tour Guide, II, pp. 25-68, Technische Universitaet Muenchen, Freising-Weihenstephan, Germany.

Bennet, J. P., 1974, Concepts of Mathematical Modeling of Sediment Yield, *Water Resources Research*, 10, 485-496.

Carslaw, H. S., and J.C. Jaeger, 1947, *Conduction of Heat in Solids*, Oxford University, London.

Desmet, P. J. J., and G. Govers, 1996, A GIS procedure for automatically calculating the USLE LS factor on topographically complex landscape units, *J. Soil and Water Cons.*, 51(5), 427-433.

Dingman, S. L., 1984, *Fluvial hydrology*, Freeman, New York.

Doe, W.W., B. Saghafian, and P.Y. Julien, 1996, Land Use Impact on Watershed Response: The Integration of Two-dimensional Hydrological Modeling and Geographical Information Systems. *Hydrological Processes*, 10, 1503-1511.

EPA, 2000, Surf your watershed; http://www.epa.org.surf2/

Flanagan, D. C., and M. A. Nearing (eds.), 1995, USDA-Water Erosion Prediction Project, *NSERL*, report no. 10, pp. 1.1- A.1, National Soil Erosion Lab., USDA ARS, Laffayette, IN.

Foster, G. R., 1982, Modeling the erosion processes, in: *Hydrologic modeling of small watersheds*, edited by C. T. Haan, H. D. Johnson, and D. L. Brakensiek, ASAE Monograph No. 5, ASAE, St. Joseph, MI, pp. 197-380.

Foster, G. R., and L. D. Meyer, 1972, A closed-form erosion equation for upland areas, in: *Sedimentation: Symposium to Honor Prof. H.A. Einstein*, edited by H. W. Shen, pp. 12.1-12.19, Colorado State University, Ft. Collins, CO.

Foster, G. R., 1990, Process-based modelling of soil erosion by water on agricultural land, in: *Soil Erosion on Agricultural Land*, edited by J. Boardman, I. D. L. Foster and J. A. Dearing, John Wiley and Sons Ltd, pp. 429-445.

Gardiner, C. W., 1985, *Handbook of Stochastic Methods for Physics, Chemistry, and the Natural Sciences*, Springer, Berlin.

Glimm J., and A. Jaffe, 1972, *Quantum Physics. A Functional Integral Point of View*, Springer, Berlin.

Govindaraju, R. S., and M. L. Kavvas, 1991, Modeling the erosion process over steep slopes: approximate analytical solutions, *Journal of Hydrology*, 127, 279-305.

Haan, C. T., B. J. Barfield, and J. C. Hayes, 1994, *Design Hydrology and Sedimentology for Small Catchments*, pp. 242-243, Academic Press.

Hairsine, P. B., and C. W. Rose, 1992, Modeling water erosion due to overland flow using physical principles 1. Sheet flow, *Water Resources Research*, 28(1), 237-243.

Hong, S., and S. Mostaghimi, 1995, Evaluation of selected management practices for nonpoint source pollution control using a two-dimensional simulation model, *ASAE*, paper no. 952700. Summer meeting of the ASAE, Chicago, IL.

Johnston, D.M. and A. Srivastava, 1999, Decision Support Systems for Design and Planning: The Development of HydroPEDDS (Hydrologic Performance Evaluation and Design Decision Support) System for Urban Watershed Planning, in: *6th International Conference on Computers in Urban Planning and Urban Management (CUPUMS'99)*, Venice, Italy (CDROM).

Julien, P. Y., B. Saghafian, and F. L. Ogden, 1995, Raster-based hydrologic modeling of spatially varied surface runoff, *Water Resources Bulletin*, 31(3), 523-536.

Karlin, S., and H. M. Taylor, 1981, *A Second Course in Stochastic Processes*, Academic Press, New York.

Kirkby, M. J., 1987, Modelling some influences of soil erosion, landslides and valley gradient on drainage density and hollow development. *Catena Supplement*, 10, 1-14.

Lettenmaier, D. P., and E. F. Wood, 1992, Hydrologic forecasting, in *Handbook of Hydrology*, edited by D. R. Maidment, pp. 26.1-26.30, McGraw-Hill, Inc., New York.

Meyer, L.D., and W. H. Wischmeier, W.H., 1969, Mathematical simulation of the process of soil erosion by water. *Transactions of the ASAE*, 12, 754-758.

Mitas, L., and H. Mitasova, 1999, Spatial Interpolation. in: *Geographical Information Systems: Principles, Techniques, Management and Applications*, edited by P.Longley, M.F. Goodchild, D.J. Maguire, D.W.Rhind, John Wiley, 481-492.

Mitas, L., and H. Mitasova, 1998, Distributed erosion modeling for effective erosion prevention. *Water Resources Research*, 34(3), 505-516.

Mitasova, H., and L. Mitas, 1999a, Modeling soil detachment by RUSLE 3d using GIS.
http://www2.gis.uiuc.edu:2280/modviz/erosion/usle.html

Mitasova, H., and L. Mitas, 1999b, Erosion/deposition modeling with USPED using GIS.
http://www2.gis.uiuc.edu:2280/modviz/erosion/usped.html

Mitasova, H., Mitas, L., Brown, W. M., and Johnston, D., 1999, *Terrain modeling and Soil Erosion Simulations for Fort Hood and Fort Polk test areas*. Report for USA CERL. University of Illinois, Urbana-Champaign, IL;
http://www2.gis.uiuc.edu:2280/modviz/reports/cerl99/rep99.html

Mitasova, H., J. Hofierka, M. Zlocha, and L.R. Iverson, 1997, Modeling topographic potential for erosion and deposition using GIS. Reply to a comment. *Int. Journal of Geographical Information Science*, 11(6), 611-618.

Mitasova, H., J. Hofierka, M. Zlocha, and L.R. Iverson, 1996, Modeling topographic potential for erosion and deposition using GIS. *Int. Journal of Geographical Information Science*, 10(5), 629-641.

Moore I.D., and Burch G.J., 1986, Modeling erosion and deposition: Topographic effects. *Transactions ASAE*, 29, 1624-1640.

Moore, I. D., and G. R. Foster, 1990, Hydraulics and overland flow, in *Process Studies in Hillslope Hydrology*, edited by M. G. Anderson and T. P. Burt, John Wiley, 215-54.

Moore, I. D., A. K. Turner, J. P. Wilson, S. K. Jensen, and L. E. Band, 1993, GIS and land surface-subsurface process modeling, in: *Geographic Information Systems and Environmental Modeling*, edited by M. F Goodchild, L. T. Steyaert, and B. O. Parks, Oxford University Press, New York, 196-230.

National Research Council, 1999, *New Strategies for America's Watersheds*, Washington DC, National Academy Press.

NSDI, 2000, *National Spatial Data Infrastructure*. http://www.nsdi.org/

Roseboom, D. and Mollahan, R., 1999, Lake Pittsfield National Monitoring Project. Report for Illinosi State Water Survey and Illinois Environmental Protection Agency, Peoria, Il.

Rouhi A., and J. Wright, 1995, Spectral implementation of a new operator splitting method for solving partial differential equations, *Computers in Physics*, 9(5), 554-563.

Saghafian, B., 1996, Implementation of a Distributed Hydrologic Model within GRASS, in *GIS and Environmental Modeling: Progress and Research Issues*, edited by M. F Goodchild, L. T. Steyaert, and B. O. Parks, GIS World, Inc., pp. 205-208.

SCS, 1988, *Manual for design of conservation measures*. Soil Conservation Service.

Srinivasan, R., and J. G. Arnold, 1994, Integration of a basin scale water quality model with GIS, *Water Resources Bulletin*, 30(3), 453-462.

Stakgold, I., 1979, *Green's Functions and Boundary Value Problems*, John Wiley, New York.

Trimble, S.W., 1999, Decreased rates of alluvial sediment storage in the Coon Creek basin, Wisconsin. *Science* 285(8), 1244-1246.

Vieux, B. E., N. S. Farajalla, and N. Gaur, 1996, Integrated GIS and distributed storm water runoff modeling, in: *GIS and Environmental Modeling: Progress and Research Issues*, edited by M. F. Goodchild, L. T. Steyaert, and B. O. Parks, GIS World, Inc., pp. 199-205.

Willgoose, G. R., and Y. Gyasi-Agyei, 1995, New technology in hydrology and erosion assessment for mine rehabilitations, *Proceedings of the APCOM XXV Conference*, Brisbane, pp. 555-562.

Willgoose, G. R., R. L. Bras, and I. Rodriguez-Iturbe, 1989, *A physically based channel network and catchment evolution model*, technical report no. 322, Ralph Parsons Lab., MIT, Cambridge, Mass., USA.

Wilson, J.P. and M.S. Lorang, 1999, Spatial Models of Soil Erosion and GIS. In Wegener M. and A.S. Fotheringham (Eds.), Spatial Models and GIS: New Potential and New Models (London: Taylor and Francis), 83-108.

Zhang Yusheng, 1999, GIS, Erosion and Deposition Modelling, and Caesium Technique. http://www.ex.ac.uk/ yszhang/welcome.htm